Pyrolysis and Oxidation of Cardboard

GAURAV AGARWAL, GANG LIU, and BRIAN LATTIMER
Department of Mechanical Engineering
Virginia Tech
203 Randolph Hall
Blacksburg, Virginia 24060 USA

ABSTRACT

Predicting the burning of cardboard requires a detailed understanding of the pyrolysis and char oxidation. An experimental study was performed to quantify the decomposition kinetics, heat of decomposition for pyrolysis, and the heat of combustion of the evolved pyrolysis gases and char oxidation. Parameters were determined using data from a simultaneous TGA / DSC as well as the microscale combustion calorimeter. From TGA data, a double independent reaction kinetic model was sufficient to describe the decomposition of cardboard due to a softened hemicellulose peak. The heat of combustion of pyrolysis gases was a factor of two less than that of the char. However, due to the lower mass loss rate of char, the heat release rate due to the char was less than half of that associated with the evolved pyrolysis gases.

KEYWORDS: Pyrolysis, Heat Release Rate, Cardboard, Kinetics, Heat of Decomposition, Heat of Combustion

NOMENCLATURE LISTING

A	pre-exponential factor (1/s)	T	temperature (^oC, K)
c	specific heat capacity (kJ/kg-K)	x_c	char conversion factor (- -)
c_{app}	apparent specific heat capacity (kJ/kg-K)	Y_c	char yield (- -)
c_{sen}	sensible specific heat capacity (kJ/kg-K)	**Greek**	
e	decomposition progress variable (- -)	β	Heating rate ($^oC/s$)
E_a	activation energy (kJ/mol)	θ	dummy integration variable
Δh_c	heat of combustion (kJ/kg)	**subscripts**	
Δh_{dec}	heat of decomposition (kJ/kg)	1	first reaction
Δh^o_{dec}	standard heat of decomposition (kJ/kg)	2	second reaction
m	instantaneous mass (kg)	a	active material
m'	time derivative of mass (kg/s)	c	char
M	mass (kg)	f	filler (ash)
n	power in kinetics models (- -)	fin	final
$\dot{Q}_{DSC}$	corrected heat flow (kW)	g	gas
$\dot{Q}_{MCC}$	heat release rate (kW)	in	initial
R	universal gas constant (8.314×10^{-3} kJ/mol-K)	p	pyrolysis gases
t	time (s)	ref	reference (298K)

INTRODUCTION

Cardboard is a common combustible material encountered in a variety of scenarios including small store rooms, box stores, and large warehouses. These commodity storage scenarios are known to be very hazardous and require sprinkler protection. Due to the cost of performing these sprinkler approval tests, there is interest in modeling the burning and suppression of commodity storage scenarios [1]. The initial ignition and flame spread in these scenarios is over surfaces of cardboard; thus, it is important to quantify the properties associated with pyrolysis and char oxidation of cardboard in order to predict the flame spread behavior. In addition, cardboard is also susceptible to smoldering which can transition into flaming. For this application, it is important to understand the energy required to generate the mass (heat of decomposition) as well as the heat produced by the smoldering, oxidizing char.

Cardboard is a material formed by delignification of soft wood (typically pine) through a process called kraft pulping. Through this process, the lignin content is reduced by 80-90% with the residual lignin chemically modified and different from the native lignin [2]. The pulp is used to form different grades of

 DOI: 10.3801/IAFSS.FSS.11-124

kraft paper including the liner and corrugated medium which are bonded together with a starch to form cardboard. Though cardboard is a lignocellulosic material, its content (provided in Table 1) is different compared to wood and paper due to the fabrication process [2]. As a result, the thermal degradation and oxidation of cardboard have been determined to be different compared with wood and paper [3-6].

Table 1. Comparison of cardboard, paper, and wood.

Material	Cellulose (%)	Hemicellulose (%)	Lignin (%)	Other (%)	HHV (kJ/kg)	Ref.
Cardboard	59.7	13.8	14.2	12.3	-14,480	[7,8]
Office Paper	64.7	13.0	0.93	21.4	-13,820	[8,9]
Newsprint	48.3	18.1	22.1	11.5	-15,870	[8,9]
Pine wood	49.8	20.8	26.7	2.7	-19,200	[10,11]

There have been limited studies that have investigated the thermal degradation and oxidation of cardboard [3, 5, 6, 8, 12]. The majority of the research performed on cardboard has been on the thermogravimetric response of cardboard in different environments (i.e., inert versus air) [3, 5, 6, 8]. No consensus has been reached on the appropriate kinetic model to predict degradation. Gupta and Muller [3] recommend first order reactions with kinetic parameters that vary with heating rate. David *et al*. [6] investigated the use of multiple reactions to predict the degradation response and found that a reaction with an intermediate product predicted the degradation best. In the work by Grammelis *et al*. [8], they used multiple independent n^{th} order reactions to predict constituent degradation (i.e. cellulose, hemicellulose, lignin). Due in part to the differences in kinetic models applied, all studies reported very different kinetic parameters. Only one study was found where they attempted to measure the heat of decomposition with values being -4,100 to -6,900 kJ/kg (exothermic) [3]. These values are overall exothermic instead of endothermic, which is different than heat of decomposition values for other fuels [13, 14]. For example, Kashiwagi and Nambu [14] found the heat of decomposition to be 570 kJ/kg for paper on a per initial mass basis.

Recently, Chaos et al. [1, 12] investigated the effects of incident heat flux and oxygen content on cardboard char oxidation. Coupon size cardboard samples were tested in the flammability apparatus in an inert environment [1] as well as in varying levels of oxygen [12]. The temperature rise of the cardboard was measured with time. After an initial transient heating period, surface temperatures remained relatively constant during the char oxidation. However, the steady state temperature changed with incident heat flux. Transient heating rates were dependent on incident heat flux and were 40°C/min at 20 kW/m^2, 600°C/min at 60 kW/m^2, 900°C/min at 100 kW/m^2. Models were proposed to predict the heat produced due to char oxidation. These resulted in effective heats of combustion ranging from 30,000-50,000 kJ/kg. Other studies have reported heat of combustion of char to range from 30,400 – 33,800 kJ/kg [12, 15].

The focus of the research presented in this paper was to quantify the thermal pyrolysis and oxidation of cardboard. Experimental methods were developed to measure individually the properties during pyrolysis as well as char oxidation. This included kinetic reaction models for pyrolysis, specific heat capacity of cardboard and char, heat of decomposition for pyrolysis, heat of combustion of the evolved pyrolysis gases, and heat of combustion of oxidizing char. A comparison of properties developed in inert environments versus oxygen containing environments is provided along with the effects of higher heating rate.

EXPERIMENTAL APPROACH

Material

The cardboard used in these experiments was a single layer of corrugated packaging cardboard shown in Fig. 1. The overall thickness was 1.7 mm with a nominal density of 315 kg/m^3. The liner thickness was 0.3 mm with the corrugated medium being 1.1 mm thick. Experiments performed in this study required 5mg samples of the cardboard. These were prepared by cutting small pieces of the cardboard that included the entire cross-section using a scalpel. Samples were conditioned at room temperature resulting in a moisture content of 8%.

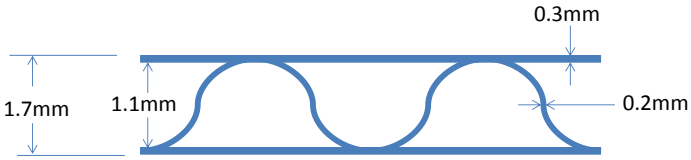

Fig. 1. Cardboard cross-sectional details.

Thermal Analysis and Calorimetry

Experiments were performed using laboratory equipment that permits relating the gravimetric, energetic, and calorimetric response to sample temperature. This allows determination of decomposition kinetics as well as simplifies determination of properties. Experiments were conducted using a simultaneous thermal analyzer (STA), which is a combination thermogravimetric analyzer (TGA) and differential scanning calorimeter (DSC), as well as a microscale combustion calorimeter (MCC).

Simultaneous Thermal Analyzer (STA)

A NETZSCH 449 F1 Jupiter STA was used to characterize the gravimetric (TGA) and energetic (DSC) response during pyrolysis and oxidation. The STA contains a platinum heater that has an operating temperature up to 1500°C and is capable of heating rates up to 50°C/min. Data from this instrument was used to determine decomposition kinetics, specific heat capacity, and heat of decomposition. An overview of the experimental method is provided here. A more detailed explanation of the calibration and operating procedures is given in a previous publication [13].

Samples for the STA were placed in 6.4 mm inner diameter Platinum-Rhodium (Pt-Rh) crucibles with Pt-Rh lids having two holes to allow the release of evolved gases. Pt-Rh crucibles were used due to their high sensitivity in DSC measurements as well as their higher operating temperatures. Lids were used to ensure that the radiation to the sample remained constant during each test and the exposure was the same on both pans. As shown in Fig. 2, the crucible containing the sample is put onto a platform inside the instrument next to an empty reference crucible and lid. The platform is connected to a load cell with a 1.0 ng resolution. The STA utilizes a differential heat flux DSC to determine the energetic response of the sample. For this, the test platform contains thermocouples to measure the pan temperature during the experiment. Based on the temperature difference, the heat flow required to heat the sample of interest is determined.

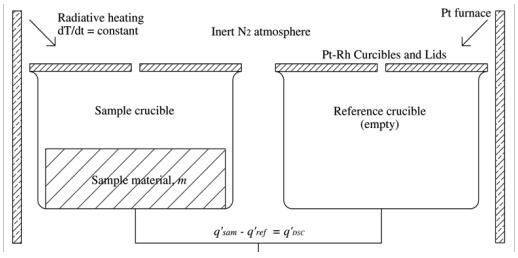

Fig. 2. Platform on the Simultaneous Thermal Analyzer (STA).

A baseline test and calibration test must be performed prior to each test to obtain quantitative data. The baseline test is performed by running the test with two sample pans on the platform with no sample in either pan. This is used to correct for the temperature effects on the load cell. Following the baseline, a calibration test is conducted using a sapphire sample in the sample pan. This is used to calibrate the heat flow with a material having a known specific heat capacity. The baseline and calibration tests were performed with the same heat rating rate, gas environment, and maximum temperature planned in the test.

Samples were tested in the mass range of 4.5 to 5.5 mg. Before and after the experiments, the initial and final sample mass was measured with an external balance having ±0.01 mg accuracy. The tests were carried out from 25°C up to 800°C to ensure complete pyrolysis and oxidation. In inert environment experiments, a nitrogen flow rate of 150 ml/min was maintained. Experiments with oxygen were conducted with 18.5%

oxygen with a total flow rate of 150 ml/min. The oxygen concentration of 18.5% was the highest possible in the instrument based on the existing configuration.

Microscale Combustion Calorimeter (MCC)

A FTT microscale combustion calorimeter (MCC) was used to measure the sample heat release rate (HRR) as a function of temperature as well as the effective heat of combustion [16,17]. Tests were performed in general accordance with ASTM E7309 [16] and Ref. [17]. The device allows the heat release rate to be related to the sample temperature as well as controlled environment combustion.

A cross-section of the instrument is shown in Fig. 3. To ensure repeatable exposure with the STA experiments, 4.5-5.5 mg samples were placed in the same Pt-Rh crucibles and lids with two holes. Before and after the experiments, the initial and final sample mass was measured with a balance having ±0.01 mg accuracy. The sample temperature was measured with a thermocouple located on the pan platform. The lower sample heater provides controlled heating of the sample (typically constant heating rate) and is capable of producing temperatures of 900°C with heating rates up to 200°C/min. The evolved gases from the sample flow up to the combustor section where a second heater is operated at a constant temperature of 900°C. The excess oxygen in the flow stream reacts with any remaining combustible gases in this section. After being cooled and water removed, the mass flow rate and oxygen concentration are measured and used to determine the heat release rate using oxygen consumption.

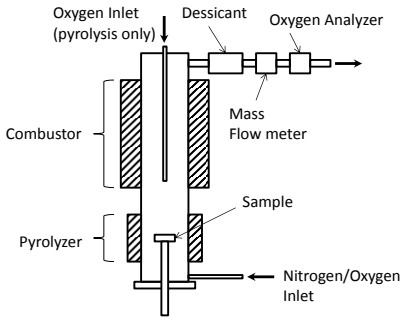

Fig. 3. Microscale combustion calorimeter (MCC).

The MCC can be used to measure the heat release rates of different stages of material burning depending on how the oxygen is introduced into the instrument. For pyrolysis in an inert environment, 80 mL/min of nitrogen was fed into the sample region and 20 mL/min of oxygen was introduced in the combustor region above the sample. In experiments with thermal degradation in an oxygen containing environment (18.5% in this study), both oxygen and nitrogen were fed into the sample region at the desired oxygen levels. In all experiments, the total flow rate was 100 mL/min. The operation requires that the oxygen sensor be calibrated and mass flow meter be checked prior to each day of testing. The oxygen sensor was calibrated with 20% oxygen.

Analysis

Kinetics

The kinetic model parameters were obtained by non-linear regression analysis on TGA data using the NETZSCH Thermokinetics software. As per the International Confederation for Thermal Analysis and Calorimetry (ICTAC) directive, non-isothermal data must be obtained at multiple heating rates to provide accurate kinetic parameters through the regression of all the data simultaneously [18]. Thus, to determine the Arrhenius kinetic parameters of cardboard pyrolysis, the STA tests were conducted at 5, 10, 20 and 40 ^{o}C/min in an inert nitrogen atmosphere to determine the cardboard gravimetric response versus temperature. The tests were conducted from 25°C up to 800°C with a two minute residence time at 800°C. Model free isoconversional methods provide reasonably accurate kinetic parameters for simple reactions which do not involve any complex reaction pathways (consecutive, parallel or independent reactions) [19].

As a result, the Friedman isoconversional model free analysis was conducted to estimate the activation energy of the reactions as well as provide insight on the number of reactions. Using the free model estimates of the activation energy and pre-exponential factor, a nonlinear regression was used to determine the final kinetic parameters [20].

Specific Heat Capacity and Heat of Pyrolysis

The specific heat capacity and heat of decomposition during pyrolysis of a sample decomposing in an inert environment were determined using the calibration corrected heat flow, $\dot{Q}_{DSC}$, from the STA. With the thermal gradient through the small sample negligible, an energy balance on the sample using the first law of thermodynamics was used to determine these properties. A detailed development of the equations below is provided elsewhere [13]. For an inert sample whose mass remains constant during heating, the sensible specific heat can be determined using the corrected heat flow using the STA by

$$c = \dot{Q}_{DSC} \big/ m\left(dT/dt\right) \tag{1}$$

where m is the mass (which remains constant) and dT/dt is the heating rate which is constant in the STA tests. If the sample undergoes thermal degradation, the sample mass changes and the energy balance must account for these changes. Energy balances for noncharring and charring materials are different since one must account for the char sensible energy during the process. The energy balances are developed in detail elsewhere [13] along with validation and measurement of properties for various materials. Since cardboard is a charring material, an overview of the energy balance equations for a charring material is presented along with the method used to determine the heat of decomposition of the sample.

A decomposing sample will contain an active (a), char (c), and inert filler part (f) producing evolved gases (g). The filler part for cardboard is ash. The energy equation was developed based on the single step reaction provided below that describes the decomposition of a fuel in an inert environment

$$active + filler \xrightarrow{\Delta 20^{o}\,\mathrm{C/min}, N_2} char + filler + gas \tag{2}$$

The initial sample mass, M_{in}, consists of the initial active mass, M_a, and the inert filler mass, M_f. Following thermal degradation in nitrogen, the constant char mass in the sample crucible is M_c while the filler part remains constant at M_f. The instantaneous mass of the sample measured during the STA experiment is the sum of all the instantaneous mass of each constituent

$$m(T) = m_a(T) + m_c(T) + M_f \tag{3}$$

where M_f remains constant due to its inert nature. Taking the derivative of this equation with respect to time provides the change in each instantaneous mass constituent,

$$m'_a(T) = \frac{1}{1 - x_c(T)} m'(T) \tag{4}$$

$$m'_c(T) = \frac{-x_c(T)}{1 - x_c(T)} m'(T) \tag{5}$$

$$m'_g(T) = -m'(T) \tag{6}$$

$$m'_f(T) = 0 \tag{7}$$

where, the char conversion factor, $x_c(T)$, is defined as

$$x_c(T) = -\frac{m'_c(T)}{m'_a(T)} = \frac{M_c}{M_a} \tag{8}$$

Thus, the char conversion factor, $x_c(T)$, is determined to be a constant value. Applying Eq. (8) onto Eqs. (4)-(7), the instantaneous mass of individual species was calculated.

From Ref [13], the energy equation for a charring material was determined to be

$$\dot{Q}_{DSC} = \left[\begin{array}{l} \left(m_a c_a + m_c c_c + m_f c_f \right) + \dfrac{dm}{dT} \\ \left(-\Delta h_{dec}^o + \dfrac{1}{1-x_c} \int_{T_{ref}}^{T} c_a dT - \dfrac{x_c}{1-x_c} \int_{T_{ref}}^{T} c_c dT - \int_{T_{ref}}^{T} c_g dT \right) \end{array} \right] \frac{dT}{dt} \tag{9}$$

where, Δh_{dec}^o in Eq. (9) represents the standard heat of decomposition per unit volatile mass lost which is not equal to the initial mass since the material chars. The standard heat of decomposition is defined as the difference in the standard heat of formations of the decomposition gas and active solid material. Hence, Δh_{dec}^o is positive for an endothermic decomposition process and is a thermodynamic property. However, this requires a reasonable estimate of the pyrolysis gases to determine the standard heat of decomposition property [13]. In this study, an effective heat of decomposition is determined as

$$\Delta h_{dec} = \Delta h_{dec}^o + \int_{T_{ref}}^{T} c_g d\theta + \frac{x_c}{1-x_c} \int_{T_{ref}}^{T} c_c d\theta - \frac{1}{1-x_c} \int_{T_{ref}}^{T} c_a d\theta \tag{10}$$

It is a positive value for a endothermic process and will be reported on per unit volatile mass loss basis, $M_a - M_c$. Though there is some variation in the effective property with sample heating rate (15% when increasing by a factor of 4), the value can be readily determined through the STA without the need for pyrolysis gas characterization. This reduces Eq. 9 to

$$\dot{Q}_{DSC} = \left[\left(m_a c_a + m_c c_c + m_f c_f \right) + \frac{dm}{dT} \left(-\Delta h_{dec} \right) \right] \frac{dT}{dt} \tag{11}$$

The heat flow is a measure of the energy required to heat up the instantaneous mass; therefore, both sides of the equation are divided by the instantaneous mass. Moving the heating rate to the left hand side, an expression is obtained relating the apparent specific heat to the sensible specific heat capacity and latent heat capacity

$$\dot{Q}_{DSC} / m \left(dT/dt \right) = c_{app} = \left(\frac{m_a c_a + m_c c_c + m_f c_f}{m_a + m_c + m_f} \right) + \frac{1}{m} \frac{dm}{dT} \left(-\Delta h_{dec} \right) \tag{12}$$

The c_{sen}, which is the first term on the right hand side of Eq. 12, can be experimentally calculated by joining the virgin sample specific heat and decomposed material specific heat values using a function based on the decomposition progress variable

$$e(T) = \frac{m(T) - M_{fin}}{M_{in} - M_{fin}} \tag{13}$$

By integrating both sides of Eq. 12 from the initial test temperature to a temperature after full decomposition is achieved, Eq. 12 can be rearranged to

$$\int_{T_{in}}^{T} \dot{Q}_{DSC} / \left(m\beta \right) dT - \int_{T_{in}}^{T} c_{sen}\, dT = -\Delta h_{dec} \ln \left(Y_c \right) \tag{14}$$

where $Y_c = M_{fin}/M_{in}$ is the char fraction and β is the heating rate. With measurements made in the STA, Eq. (14) can be used to determine the heat of decomposition. This has been validated elsewhere [13, 21]. Based on error analysis including machine accuracy and repeatability, the heat of decomposition was determined to have an uncertainty of ±4.9%.

Effective Heat of Combustion

The heat release rate measured in the MCC was used to determine the effective heat of combustion of the sample. From the MCC, the heat release rate is expressed on a per initial mass basis and can be related to the mass loss rate and heat of combustion through

$$\dot{Q}_{MCC}/M_{in} = \frac{1}{M_{in}}\frac{dm}{dt}\Delta h_c \tag{15}$$

The effective heat of combustion is determined through integrating both sides with respect to time and solving for the heat of combustion. Since the heat release rate is measured with respect to temperature, it is convenient to use the chain rule to change the integration variable to temperature. This results in the following equation to calculate the effective heat of combustion

$$\Delta h_c = \frac{1}{\beta\left(1-Y_c\right)}\int_{T_{in}}^{T}\frac{\dot{Q}_{MCC}}{M_{in}}d\theta \tag{16}$$

This has been validated elsewhere [21]. Based on error analysis including machine accuracy and repeatability, the heat of combustion was determined to have an uncertainty of ±3.5%.

Test Matrix

Experiments were performed in different environments to determine the properties during pyrolysis, char oxidation, and thermal oxidation degradation of a sample. Table 2 contains a summary of the experimental conditions used to determine different properties.

Table 2. Tests performed in the study.

Property	Sample	Instrument	Environment	Heating rate (^oC/min)
Kinetic Parameters, A, E_a, n	5 mg Cardboard[a]	STA and MCC	Nitrogen	5, 10, 20, 40 (STA) 20, 100 (MCC)
Δh_{dec}	5 mg Cardboard	STA	Nitrogen	20
$\Delta h_{c,p}$	5 mg Cardboard	MCC	Nitrogen	20
$\Delta h_{c,c}$	5 mg Char[b]	MCC	18.5% O_2	20
Δh_c	5 mg Cardboard	MCC	18.5% O_2	20

[a]MCC sample masses decreased to 3 mg at 100°C/min to ensure uniform sample heating
[b]Char formed from inert heating of 24 mg of cardboard in nitrogen at 20°C/min to a temperature of 440°C for Case 1 and to a temperature of 800°C in Case 2 .

The kinetic parameters for decomposition in an inert environment were determined with a series of tests in the STA at heating rates of 5, 10, 20, and 40 ^{o}C/min. Higher heating rate pyrolysis at 100 ^{o}C/min was quantified through tests in the MCC by dividing the heat release rate curve by the effective heat of combustion. Based on the surface temperature data in Ref. [12], this heating rate approximately corresponds to the temperature rise of cardboard when exposed to a heat flux of 20-30 kW/m^2.

The heat of decomposition for pyrolysis, Δh_{dec}, in an inert atmosphere was measured using the STA with a nitrogen environment operating at 20°C/min. Using the gravimetric and heat flow data, the heat of decomposition was determined using Eqn. 14.

The effective heat of combustion was determined for the evolved pyrolysis gases ($\Delta h_{c,p}$), char oxidation ($\Delta h_{c,c}$), and thermal oxidation degradation (Δh_c) of a sample through a series of tests in the MCC. Using Eq. 16, the effective heat of combustion was determined through the heat release rate measured as a function of sample temperature in the MCC. To determine the pyrolysis gas effective heat of combustion, the sample was pyrolyzed in nitrogen and the evolved gases were burned in the combustor inside the MCC. To determine the effective heat of combustion for the char, a char sample was prepared by pyrolyzing 24 mg of cardboard in an inert environment at 20°C/min up to a temperature after the majority of pyrolysis had completed (440°C) as well as nearly full completion of pyrolysis (800°C). The char sample was allowed to cool back to room temperature and reweighed. The char weight ranged from 5-6 mg. The char sample was then reheated in the MCC at 20°C/min in 18.5% oxygen to determine the heat release rate of the char only.

Lastly, cardboard samples were tested in 18.5% oxygen at 20°C/min to determine the heat release rate including both pyrolysis and char oxidation.

RESULTS AND DISCUSSION

Pyrolysis Behavior

Experimental results are provided in Fig. 4 for cardboard undergoing thermal degradation in nitrogen in the STA and the MCC. In these plots, all data are provided on a per initial mass basis with positive DSC values representing an endothermic process.

In Fig. 4a, the mass fraction starts at 0.94 of the initial mass due to the vacuum cycling drawing moisture out of the sample prior to heating. Upon heating, the initial drop in the mass at 100°C is due to the remaining moisture being driven off from the sample. The primary decomposition occurs from 250-400°C with a more gradual decomposition continuing at temperatures above 400°C. This is different compared to wood which has three distinct decomposition regions associated with decomposition of hemicellulose, cellulose and lignin [4,11]. For cardboard, the first peak is associated with the decomposition of both hemicellulose and cellulose; however, the hemicellulose peak is softened. This is attributed to both the kraft process reducing the hemicellulose content as well as the sulfates from this process in the cardboard being catalyst for the early reaction of the cellulose making the hemicellulose peak less pronounced [5]. The second more gradual decomposition above 400°C is attributed to the degradation of lignin. The decomposition of hemicellulose and cellulose is endothermic while lignin decomposition to char is slightly exothermic (seen between 400-500°C), which is similar to that reported elsewhere [22, 23]. Based on Eq. 14 and the measured char yield of 0.198, the heat of decomposition for pyrolysis in nitrogen was determined to be 117 kJ/kg on a per active mass basis.

The heat release rate of the pyrolysis gases is shown in Fig. 4b to take on a shape similar to that of the DTG curve, as expected. In addition, the peak values occur at approximately 370°C. This indicates that the decomposition occurring in the STA and MCC are similar. Using Eq. 16 and a char yield of 0.183 from the MCC experiment, the effective heat of combustion of the pyrolysis gases was determined to be -13,610 kJ/kg and exothermic.

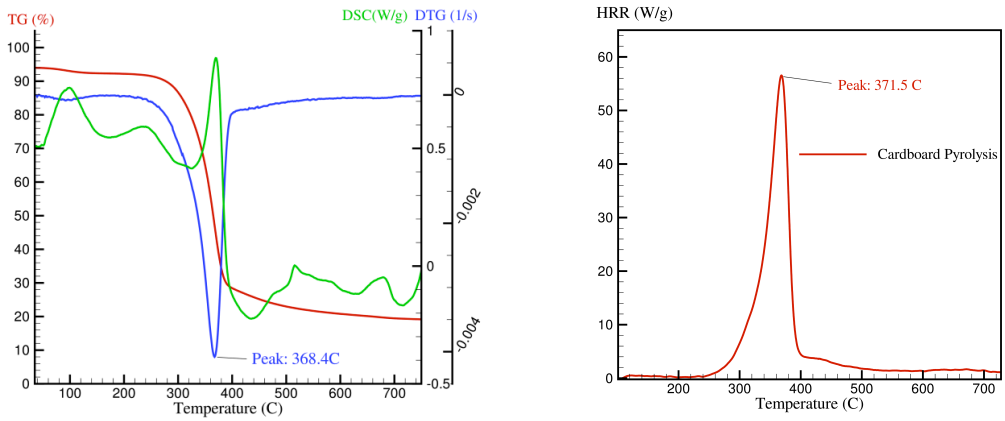

(a) (b)

Fig. 4 Thermal degradation in nitrogen at 20°C/min including the a) mass loss, heat flow and mass loss rate from the STA; and b) heat release rate of the pyrolysis gases from the MCC.

Pyrolysis Kinetics

The kinetic models and parameters for cardboard were developed using data at four different heating rates from the STA (5, 10, 20, and 40°C/min). To determine the kinetic parameters, nonlinear regression analysis was performed on all of the heating rate data simultaneously to ensure an optimized fit over the tested heating rates. The Friedman isoconversion analysis was used to investigate the nature of cardboard pyrolysis kinetic mechanism, and the results are shown in Fig. 5. The slopes of the isoconversional lines are the activation energy. The slope in the lines from α=0.02-0.70 are similar indicating one type of reaction

over this range, while a separate reaction at α>0.70 is indicated by the different line slope in this range. The slope of measured values at the start of the reaction (1000/T = 1.9) is less than the slope of isoconversion lines (α=0.02-0.70). Based on Ref. [19], the higher slope for the isoconversion lines at α=0.02-0.70 indicates a diffusion type reaction.

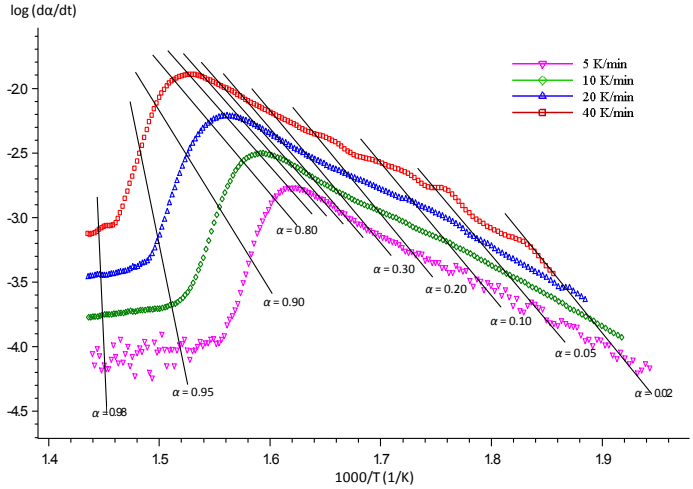

Fig. 5. Friedman analysis on gravimetric data for cardboard pyrolysis at different heating rates.

To further investigate this assumption, non-linear regression analysis was used to calculate the Arrhenius kinetic parameters of different reaction models. The kinetic parameters obtained from non-linear regression analysis provide a best fit to the assumed kinetic model, irrespective of the complexity of the kinetics involving multiple consecutive, parallel or independent reactions [20]. In addition, the change in slopes also indicates that more than one reaction will be required to predict the decomposition. Initial estimates of the activation energies and pre-exponential factors were determined from the model-free isoconversional Friedman analysis on all of the data. In models with a power, the value of *n* was initially set to 1 but limited to 3 to prevent unrealistically large powers. Perturbing these initial estimates did not affect the final nonlinear regression result.

The different kinetic models evaluated in this work are provided in Table 3. The reaction models are listed in decreasing order of fit quality with $F_{exp} = 1$ being the best fit. This included single step reactions as well as various two step reactions. As expected from the model free analysis, the single reaction models did not represent the data well resulting in high F-test correlation values. The investigated models for the double reaction approach included independent, parallel, competitive and consecutive reaction models.

As observed from Table 3, the double independent reaction model provided the best prediction of the cardboard pyrolysis data. The first reaction was a diffusion reaction, which was selected based on the isoconversional analysis, while the second was a nth order reaction. This is different than that in the literature where multiple n^{th} order reaction models are proposed [3, 6, 8]. The pre-exponential factor (*A*), activation energy (E_a) and reaction order (*n*) for each of these two decomposition reactions was obtained using non-linear regression analysis. Table 4 contains the kinetic parameters for the two independent reaction model. Fig. 6 contains the double independent model prediction compared with the cardboard pyrolysis data, showing excellent agreement with the experimental data.

The subscripts '1' and '2' represent the parameters for the two dimensional diffusion reaction and n^{th} order reaction models, respectively. The independent diffusion reaction model best represents the decomposition of the hemicellulose and cellulose. This can be represented as a single reaction due to the hemicellulose peak being subdued, as previously described. The A_1 and E_{a1} values calculated using this model are close to the Arrhenius kinetic parameters for cellulose decomposition obtained for cardboard [5,6], kraft paper [22], and paper [14]. The second reaction is an nth order decomposition reaction that represents the lignin decomposition reaction. During the kraft process, the lignin is chemically modified and is different than the native lignin in the pine wood [2]. As a result, the Arrhenius parameters for lignin decomposition in cardboard were found to be different than those reported for biomass samples [11]. This is attributed to the reduction and modification of the lignin through the kraft process.

Table 3. F-Test for non-linear regression fit using different reaction models. F_{crit} (0.95) = 1.11

Reaction type	Reaction model	$f(\alpha)$*	F_{exp}	Variables
Double independent	$A \xrightarrow{1,D_2} Gas1$ $B \xrightarrow{2,F_n} Gas2$	$F_n : (1-\alpha)^n \; D_2 : -1/\ln(1-\alpha)$	1.00	6
Double consecutive	$A \xrightarrow{1,D_2} B + Gas1$ $B \xrightarrow{2,F_n} Gas2$	$F_n : (1-\alpha)^n \; D_2 : -1/\ln(1-\alpha)$	1.77	6
Double competitive	$A \xrightarrow{1,D_2} Gas1$ $A \xrightarrow{2,F_n} Gas2$	$F_n : (1-\alpha)^n \; D_2 : -1/\ln(1-\alpha)$	2.72	6
Double parallel	$A \xrightarrow{1,D_2} Gas1$ $A \xrightarrow{2,F_n} Gas1$	$F_n : (1-\alpha)^n \; D_2 : -1/\ln(1-\alpha)$	3.92	6
Single 2D diffusion	$A \xrightarrow{1,D_2} Gas$	$D_2 : -1/\ln(1-\alpha)$	4.87	2
Single 3D diffusion	$A \xrightarrow{1,D_3} Gas$	$D_3 : \dfrac{1.5}{(1-\alpha)^{-1/3} - 1}$	5.02	2
Single 1D diffusion	$A \xrightarrow{1,D_1} Gas$	$D_1 : 0.5/\alpha$	8.97	2
Single nth-order	$A \xrightarrow{1,F_n} Gas$	$F_n : (1-\alpha)^n$	25.64	3

$$* \frac{d\alpha}{dt} = k(T) f(\alpha) = A \exp\left(-\frac{E_a}{RT}\right) f(\alpha)$$

Table 4. Arrhenius reaction parameters for two independent reaction model.

Parameters	Initial values from Friedman analysis	Optimized values from non-linear regression
log A_1 (s^{-1})	13.5	13.00
E_{a1} (kJ/mol)	187.00	184.92
log A_2 (s^{-1})	15.0	15.70
E_{a2} (kJ/mol)	206.0	214.68
n_2	1	2.29
Fraction Mass $Loss_1$	0.84	0.78
Fraction Mass $Loss_2$	0.16	0.22

The fraction mass loss in Table 4 represents the fraction of mass loss from the initial mass due to each decomposition reaction. As observed from Table 4 and Fig. 6, the majority of the mass loss from the cardboard sample was associated with the cellulose and hemicellulose decomposition while a lower fraction of the mass loss was due to the lignin decomposition reaction.

The kinetic model based on nonlinear regression of STA data at four heating rates was used to predict the mass loss rate of samples in the MCC at heating rates of 20°C/min and 100°C/min. The lower heating rates of 5-40°C/min are consistent with small incipient fire exposures, such as those that may be present for smoldering combustion or very small flames. The higher heating rate of 100°C/min is closer to but on the low side of what would be expected in higher heat flux fire exposures. The mass loss rate data was developed by dividing the heat release rate by the effective heat of combustion. The prediction of the high

heating rate data is provided in Fig. 6b. The model predicted the mass loss rate from the MCC data at 20 °C/min but the predicted mass loss rate at a 100 °C/min was shifted in temperature. This indicates that higher heating rate data should be included in nonlinear regression analysis to determine the kinetic parameters to ensure better scaling.

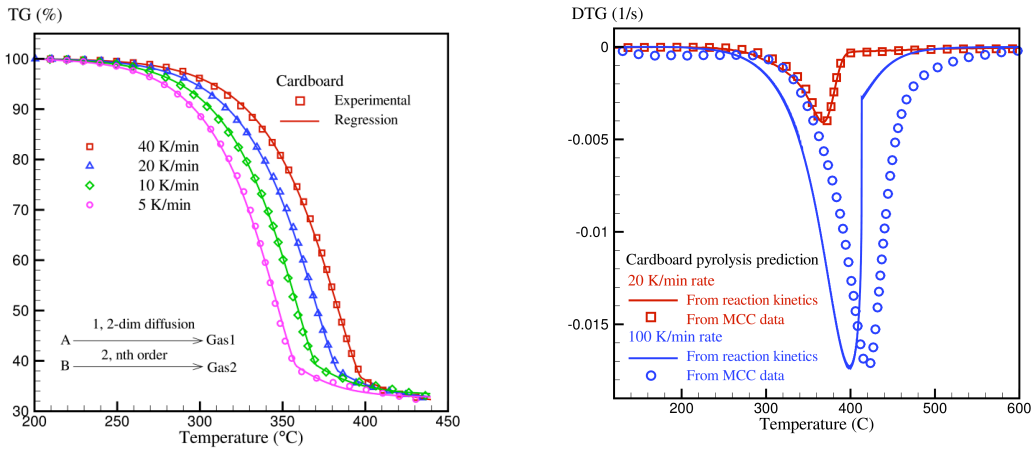

(a) (b)

Fig. 6 Cardboard pyrolysis data compared with the double independent reaction model from data in the a) STA and b) MCC.

Thermal Oxidation of Char

The thermal oxidation of char was quantified through testing in both the STA and MCC. The results of the tests are provided in Fig. 7 for char formed through two different methods. In one case, the char was formed by decomposing cardboard in an inert environment up to 440°C just after decomposition of the hemicellulose and cellulose, which is the majority of the decomposition. This was done to better represent the char that oxidizes when the cardboard is thermally oxidized. The second method for char formation was performed by heating the sample to 800°C for complete pyrolysis of the sample. This case best represents the char product.

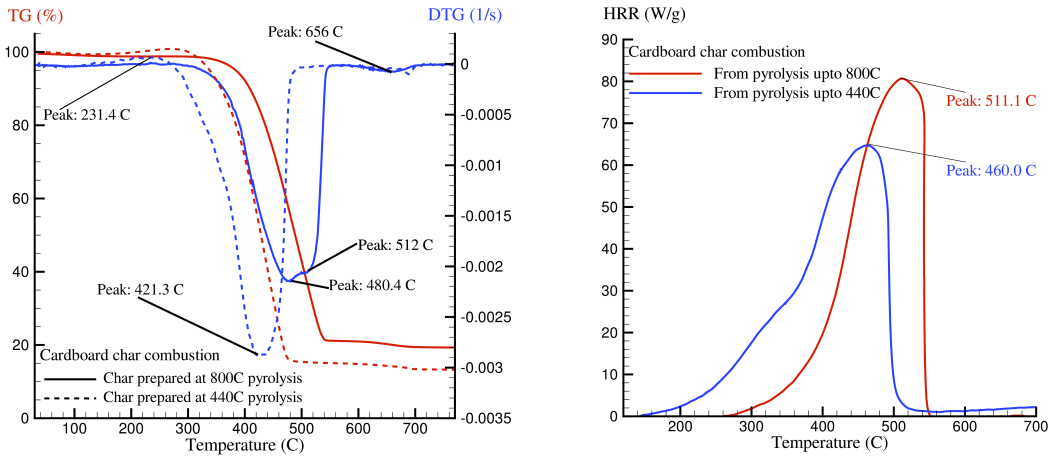

(a) (b)

Fig. 7. Thermal oxidation of chars in 18.5% oxygen at 20°C/min including the a) gravimetric response in the STA and b) heat release rate from the MCC.

As seen in Fig. 7, the two chars do not decompose in the same manner. The char formed through heating to a lower temperature (440°C) was more reactive. This was expected due to the likely presence of lignin in the sample. In addition, the low temperature char also displayed a chemiabsorption between 250-350°C. This has also been observed in coal samples [21]. The lower temperature char was measured to have a

peak DTG and heat release rate at 460°C compared with 510°C for the char formed at higher temperatures. In addition, the char formed at lower temperature (which was more reactive) had a lower peak heat release rate compared with the char formed at higher temperature. Despite these differences, both chars were measured to have similar effective heat of combustion values. The char formed at lower temperatures had an effective heat of combustion of -32,860 kJ/kg while the char formed at higher temperature had a value of -34,070 kJ/kg. Note these values are per active mass of the char. These values compare well with the char values of -30,400 to -33,800 kJ/kg reported elsewhere [12, 15].

Thermal Oxidation of Cardboard

Measurements were also performed on cardboard in 18.5% oxygen. In these tests, the sample undergoes pyrolysis and char oxidation. The gravimetric and heat release rate response of these samples is provided in Fig. 8. The initial peak is the pyrolysis of the hemicellulose and cellulose, which is responsible for the largest mass loss rate and heat release rate. In the presence of oxygen, these peaks occur at lower temperatures compared with the mass loss rate and heat release rate peaks for pyrolysis only in nitrogen as shown in Fig. 4b. This was attributed to the change in the kinetic decomposition mechanism for the cellulose [14]. Although the mass loss rate during lignin pyrolysis and char oxidation is an order of magnitude lower than the hemicellulose / cellulose decomposition, the heat release rate is only a factor of two less than the heat release rate of the hemicellulose / cellulose peak. This was attributed to the char having an effective heat of combustion a factor of three higher than that of the hemicellulose / cellulose. The effective heat of combustion for the thermal oxidation of cardboard was determined to be -16,200 kJ/kg.

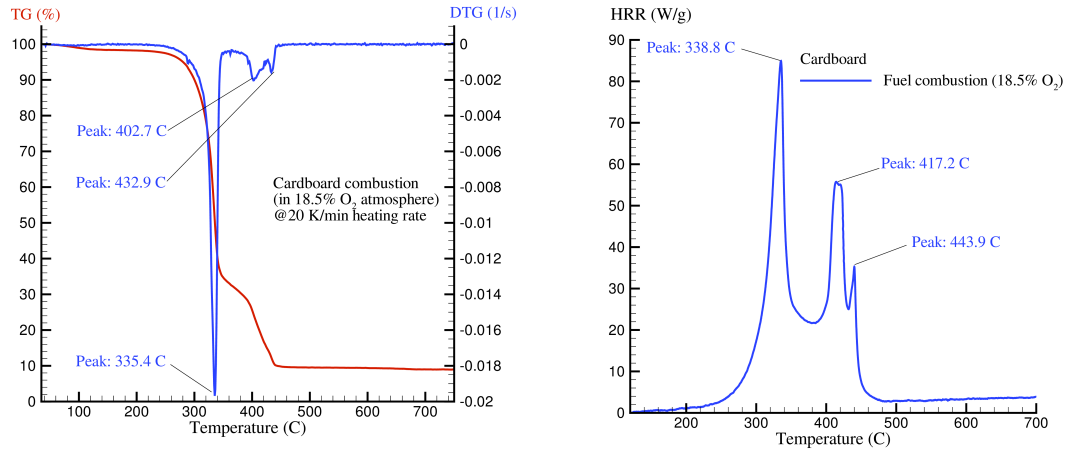

(a) (b)

Fig. 8. Thermal oxidation of cardboard in 18.5% oxygen at a heating rate of 20°C/min including the a) gravimetric response in the STA and b) heat release rate in the MCC.

Table 5 contains all of the effective heats of combustion measured in the study with the MCC. In addition, the effective heat of combustion of the cardboard was measured using the cone calorimeter to be 13,500 ± 1,900 kJ/kg and is provided in the Table 5. The value measured using the cone calorimeter was lower than that from the MCC. This may be in part due to the MCC having a more complete combustion due to the combustor downstream of the sample compared with the cone calorimeter. The effective heat of combustion due to pyrolysis gases and char oxidation individually were used to determine the effective heat of combustion for the thermal oxidation of the cardboard. Since each effective heat of combustion value is on an active mass basis, the effective heat of combustion for thermal oxidation of cardboard was determined from the pyrolysis gas and char components by

$$\Delta h_c = \Delta h_{c,p}\left(1 - Y_c\right) + \Delta h_{c,c} Y_c \tag{17}$$

The char yield was taken from the pyrolysis experiment in the MCC as Y_c=0.183. The results of this analysis are shown in Table 5. The predicted effective heats of combustion are within 7% of the value measured using the MCC.

Table 5. Measured and predicted effective heat of combustion of cardboard.

Δh_c Measured (kJ/kg)[a]					Δh_c Predicted (kJ/kg)	
Pyrolysis Gases	Char Oxid. Case 1[b]	Char Oxid. Case 2[b]	Cardboard Oxidation	Cone Calorimeter	Pyrol+Char Case 1	Pyrol+Char Case 2
-13,610	-32,860	-34,070	-16,200	-13,500	-17,130	-17,350

[a]All values from the MCC except cone calorimeter
[b]Char formed from inert heating of 24 mg of cardboard in nitrogen at 20°C/min to a temperature of 440°C for Case 1 and to a temperature of 800°C in Case 2

CONCLUSIONS

An experimental study was conducted to utilize new techniques and instruments to quantify some properties for predicting the pyrolysis and oxidation of cardboard. Energy balance equations were used to provide a framework to use TGA, DSC and MCC data to determine pyrolysis and oxidation properties of cardboard. The pyrolysis was determined to consist of double independent reactions due to the subdued hemicellulose peak and decrease in amount of hemicellulose. This kinetic model was demonstrated to be capable of predicting the gravimetric response over the range it was developed, but resulted in a curve shifted from the data at higher heating rates (100°C/min). The heat of decomposition for pyrolysis was determined to be 117 kJ/kg. The effective heat of combustion of the pyrolysis gases was determined to be -13,610 kJ/kg while the char oxidation had an effective heat of combustion of -32,860 to -34,070 kJ/kg. Despite the dramatic differences in heats of combustion, the pyrolysis gases were measured to have the larger contribution to the cardboard heat release rate in an oxygen containing environment due to the higher mass loss during pyrolysis. The effective heat of combustion of cardboard during thermal oxidation was -16,200 kJ/kg, which could be predicted through the fractional sum of the pyrolysis gas and char oxidation effective heats of combustion.

ACKNOWLEDGEMENTS

This work was supported by the Virginia Tech Institute of Critical Technology and Applied Science (ICTAS).

REFERENCES

[1] M. Chaos, M. M. Khan, N. Krishnamoorthy, J. L. de Ris, and S. B. Dorofeev, "Evaluation of optimization schemes and determination of solid fuel properties for CFD fire models using bench-scale pyrolysis tests," *Proceedings of the Combustion Institute*, 33(2) : 2599–2606, 2011. http://dx.doi.org/10.1016/j.proci.2010.07.018

[2] I. a. Weinstock, R. H. Atalla, R. S. Reiner, M. a. Moen, K. E. Hammel, C. J. Houtman, C. L. Hill, and M. K. Harrup, "A new environmentally benign technology for transforming wood pulp into paper. Engineering polyoxometalates as catalysts for multiple processes," *Journal of Molecular Catalysis A: Chemical*, 116 (1–2) : 59–84, 1997. http://dx.doi.org/10.1016/S1381-1169(96)00074-X

[3] A. K. Gupta and P. Muller, "Pyrolysis of Paper and Cardboard in Inert and Oxidative Environments," *Journal of Propulsion and Power*, 15(2) : 187–194, 1999. http://dx.doi.org/10.2514/2.5441

[4] C. Di Blasi, "Modeling chemical and physical processes of wood and biomass pyrolysis," *Progress in Energy and Combustion Science*, 34(1) : 47–90, 2008. http://dx.doi.org/10.1016/j.pecs.2006.12.001

[5] L. Sùrum, M. G. Grùnli, and J. E. Hustad, "Pyrolysis characteristics and kinetics of municipal solid wastes," *Fuel*, 80 : 1217–1227, 2001. http://dx.doi.org/10.1016/S0016-2361(00)00218-0

[6] C. David, S. Salvador, J. L. Dirion, and M. Quintard, "Determination of a reaction scheme for cardboard thermal degradation using thermal gravimetric analysis," *Journal of Analytical and Applied Pyrolysis*, 67(2): 307–323, 2003. http://dx.doi.org/10.1016/S0165-2370(02)00070-0

[7] R. Yáñez, J. . Alonso, and J. . Parajó, "Production of hemicellulosic sugars and glucose from residual corrugated cardboard," *Process Biochemistry*, 39(11): 1543–1551, 2004. http://dx.doi.org/10.1016/S0032-9592(03)00283-8

[8] P. Grammelis, P. Basinas, a. Malliopoulou, and G. Sakellaropoulos, "Pyrolysis kinetics and combustion characteristics of waste recovered fuels," *Fuel*, 88(1):195–205, 2009. http://dx.doi.org/10.1016/j.fuel.2008.02.002

[9] Y. Chen, D. R. U. Knappe, and M. a Barlaz, "Effect of cellulose/hemicellulose and lignin on the bioavailability of toluene sorbed to waste paper," *Environmental science & technology*, 38(13): 3731–6, 2004. http://dx.doi.org/10.1021/es035286x

[10] DiNenno, P.J. "Appendices," *The SFPE Handbook of Fire Protection Engineering (3rd ed),* DiNenno P.J. (ed.), National Fire Protection Association, Quincy, MA 02269, 2002, p. A-42.

[11] M. Müller-Hagedorn, H. Bockhorn, L. Krebs, and U. Müller, "A comparative kinetic study on the pyrolysis of three different wood species," *Journal of Analytical and Applied Pyrolysis*, 68–69: 231–249, 2003. http://dx.doi.org/10.1016/S0165-2370(03)00065-2

[12] M. Chaos, M. M. Khan, and S. B. Dorofeev, "Pyrolysis of corrugated cardboard in inert and oxidative environments," *Proceedings of the Combustion Institute*, 34(2): 2583–2590, 2013. http://dx.doi.org/10.1016/j.proci.2012.06.031

[13] G. Agarwal and B. Lattimer, "Method for measuring the standard heat of decomposition of materials," *Thermochimica Acta*, 545:34–47, 2012. http://dx.doi.org/10.1016/j.tca.2012.06.027

[14] T. Kashiwagi and H. Nambu, "Global kinetic constants for thermal oxidative degradation of a cellulosic paper," *Combustion and Flame*, 88(3–4):345–368, 1992. http://dx.doi.org/10.1016/0010-2180(92)90039-R

[15] S. A. Channiwala and P. P. Parikh, "A unified correlation for estimating HHV of solid , liquid and gaseous fuels," *Fuel*, 81:1051-1063, 2002. http://dx.doi.org/10.1016/S0016-2361(01)00131-4

[16] ASTM E7309-11, "Standard Test Method for Determining Flammability Characteristics of Plastics and Other Solid Materials Using Microscale Combustion Calorimetry," ASTM International, 2013.

[17] Lyon, R., Walters, R., Staliarov, S., and Safronava, N., "Principles and Practice of Microscale Combustion Calorimetry," FAA Draft Report, FAA, Atlantic City, NJ, 2012.

[18] Burnham, A. K., "Computational aspects of kinetic analysis.: Part D: The ICTAC kinetics project — multi-thermal–history model-fitting methods and their relation to isoconversional methods," Thermochimica Acta, 355(1–2):165-170, 2000. http://dx.doi.org/10.1016/S0040-6031(00)00446-9

[19] Opfermann, J. R., Kaisersberger, E., and Flammersheim, H. J., 2002, "Model-free analysis of thermoanalytical data-advantages and limitations," *Thermochimica Acta*, 391(1–2), pp. 119-127. http://dx.doi.org/10.1016/S0040-6031(02)00169-7

[20] Opfermann, J., "Kinetic Analysis Using Multivariate Non-linear Regression. I. Basic concepts," *Journal of Thermal Analysis and Calorimetry*, 60(2):641-658, 2000. http://dx.doi.org/10.1023/A:1010167626551

[21] Agarwal, G., Liu, G., and Lattimer, B., "Pyrolysis and Combustion Energetic Characterization of Coal-Biomass Fuel Blends," POWER2013-98313, ASME, Boston, MA, 2013, 10p.

[22] S. Soares, G. Caminot, and S. Levchik, "Comparative study of the thermal decomposition of pure cellulose and pulp paper," *Polymer Degradation and Stability*, 49:275–283, 1995. http://dx.doi.org/10.1016/0141-3910(95)87009-1

[23] M. Statheropoulos, S. Liodakis, N. Tzamtzis, a. Pappa, and S. Kyriakou, "Thermal degradation of Pinus halepensis pine-needles using various analytical methods," *Journal of Analytical and Applied Pyrolysis*, 43(2):115–123, 1997. http://dx.doi.org/10.1016/S0165-2370(97)00064-8